Paper No. 236

ISMS 2016

Quantitative analysis of haulage system instability in deep hard rock mines using numerical modelling

Shahé Shnorhokian [a,*], Bryce MacNeil [a], Hani Mitri [a]

[a] Department of Mining and Materials Engineering, McGill University, Montreal (QC), Canada, H3A 0E8

ABSTRACT
Haulage drifts and related infrastructure are crucial to the success of underground mining operations. In the sublevel stoping mining method, they are developed well before any extraction commences in a given section of the orebody. One of the more complex design parameters is the relative distance of a haulage drift from the orebody as it runs parallel to its strike. Opposing considerations from operational and ground control teams need to be balanced, with the former preferring a shorter distance for increased productivity and the latter requesting a further distance for safety and stability. Numerical codes are one of the analytical tools used frequently in making these decisions by providing mining-induced stress and displacement magnitudes using a properly calibrated model. In this study, a simplified model is constructed of a typical tabular orebody within the geological settings of the Canadian Shield, striking East-West and dipping steeply to the south. Three other formations with the same strike and dip are added to the model, along with two intrusive dykes at variable distances from the orebody and the drift. The rockmass properties for all formations are obtained from a previous work on a case study mine in the Canadian Shield, and the model is calibrated based on in-situ stress measurements there. Two stope sequences comprising two simultaneous mining fronts are implemented and analyzed for the orebody; a diminishing pillar one that moves from both east and west to the middle, and a center-out option that moves from its center to the sides. In both cases, 24 mine-and-backfill stages – comprising 6 stopes each – are needed to completely extract the orebody. A quantitative assessment of instability around the drifts, crosscuts, and stopes is conducted at each stage for a level at a depth of 1490 m. Two instability parameters – the brittle shear ratio (BSR) and a low compressive-tensile stress state – are combined with volumetric analysis to obtain the quantity of potentially unstable rockmass. The relative proximity of the drift and stopes to the dykes is evaluated and observed to have an impact on the results. A combined numerical-volumetric approach is found to provide a useful tool for comparing different sequences and obtaining information on the type, location, volume, and timing of rockmass instability.
KEYWORDS: drift instability; modelling; stope sequence; brittle shear ratio; low compressive-tensile stress

1. INTRODUCTION

Haulage drifts, crosscuts, and the intersections they form constitute a vital component of operations in underground hard rock mines. They are especially crucial for certain mining methods such as sublevel open stoping where considerable resources need to be allocated at the onset of operations to develop them (Hamrin, 1998; Bullock, 2011). Hence, it is crucial that they remain stable for an extended period of time while mining is conducted in a certain area. The distance of the haulage drift from the stopes requires an informed and experienced decision able to satisfy two opposing requirements. On one hand, it needs to be as close to the orebody as possible to optimize ore haulage activities. On the other hand, it needs to be far enough from the stopes so as not to be influenced by stress redistributions resulting from ore extraction. The literature is rich with studies that have examined drift stability using a number of techniques such as instrumentation and monitoring (Kendorski, 1993; Kaiser et al., 2001; Diederichs et al., 2004), and numerical approaches (Martin et al., 1999; Zhang and Mitri, 2008; Cai and Kaiser, 2014). Empirical methods used for drift stability and support design constitute the basis of several rockmass classification schemes (Bieniawski, 1989; Grimstad and Barton, 1993; Hoek et al., 2002). Kaiser et al. (2000) provide an extensive summary of the different approaches available for drift stability analysis. One of the fundamental concerns in deep hard rock mines is the occurrence of rockbursts that pose safety concerns to personnel and cause severe damage to the network of drifts and crosscuts. A number of recommendations on different mitigation and support measures have been presented over the years (Gay et al., 1995; Kaiser et al., 1996; Cai, 2013).

Numerical modelling provides a useful analytical tool for determining design parameters such as the optimum distance of the drift from the stopes while satisfying the criteria mentioned above. In addition to

*Corresponding author – email : shahe.shnorhokian@mail.mcgill.ca

calculating induced stresses and displacements, it can compare the merits of several stope sequences based on the location and relative timing of any potential instability. Starting with the geometry and rockmass properties of the formations, an instability criterion can be combined with simple volumetric analysis for a quantitative assessment of stope extraction options.

In this study, a conceptual model is constructed with the finite difference code FLAC^{3D} (Itasca, 2006) to represent a typical underground hard rock metal mine in the Canadian Shield. A combination of volumetric analysis and two instability indicators – the brittle shear ratio (BSR) and a low compressive-tensile stress state – are used to quantitatively assess potential ground control issues in drifts, crosscuts, and intersections for a level at a depth of 1490 m.

2. MODEL SETUP

The model is constructed in FLAC^{3D} to replicate typical geological conditions in the Canadian Shield, comprising several formations with east-west strikes and dips of approximately 80° to the south. A central greenstone formation hosts the orebody and typical igneous intrusions in the area are represented by two dykes trending WNW-ESE and running sub-parallel to the orebody. Based on its geometry and strike, the north dyke is at a further distance from the haulage drift in the western part of the mine. Inversely, the south dyke is closer to the orebody in the western part and moves away from it in the east. The variable proximity of the dykes to the drifts and orebody is used to examine their impact on mining-induced stresses and associated potential instability.

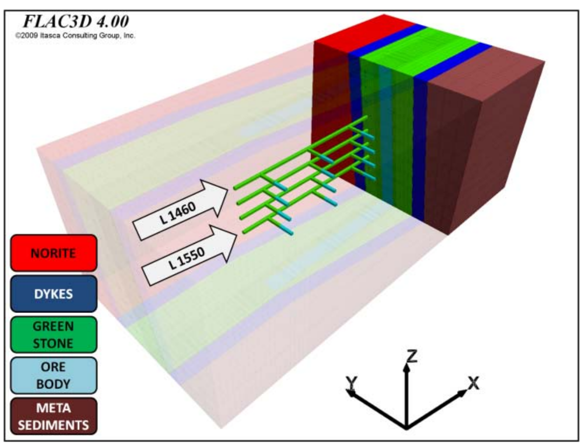

Figure 1: 3D view of numerical model with geological formations and drift-crosscut system on active levels.

The orebody is tabular in shape, and extends 360 m in the E-W direction with a thickness of 30 m in the N-S direction. Four active levels – L 1550, L 1520, L 1490, and L 1460 – are set up at depths between 1430 m to 1550 m (120 m in height), along with extensions in all three axis directions to have the model boundaries far from any openings created by mining activities. Each level includes 32 stopes with individual L × W × H dimensions of 20 × 15 × 30 m for a volume of 9000 m^3 per stope.

The final model dimensions of are 840 m (E-W), 390 m (N-S), and 300 m in depth. A total of 862000 zones are generated with the mesh density increasing in the areas of study. Figure 1 presents the general layout of the mine and the geological formations.

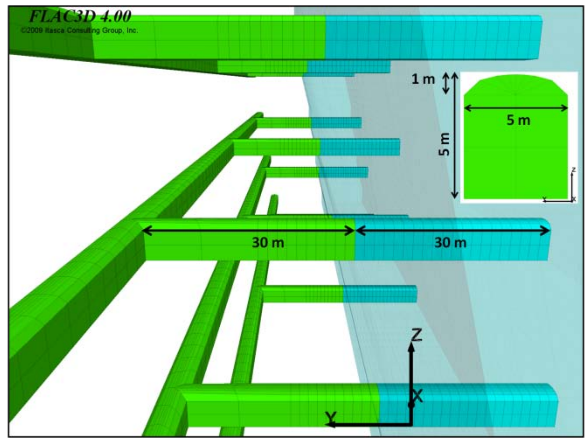

Figure 2: Close-up view of drift-crosscut system on L 1490.

Haulage drifts are constructed in the footwall of each of the four active levels at a constant distance of 30 m from – and parallel to – the orebody. From the drift, three perpendicular crosscuts 60 m in length are extended to the orebody, with the initial 30 m within the greenstone footwall and the remaining segment cutting into the stopes. These are 120 m apart along the strike and similar to the drifts, they measure 5 × 5 m in cross-section with an arch of 1 m at the center of the roof. A drift-crosscut intersection is presented in Figure 2 along with a typical cross-sectional view.

The input rockmass properties for the model are based on previous publications by the authors for a case study mine in the Canadian Shield (Shnorhokian et al 2015). They are presented in Table 1 for all the formations in this study.

Table 1: Input rockmass properties for numerical model.

Geological formation	Density (kg/m^3)	Bulk K (GPa)	Shear G (GPa)	UCS (MPa)
Norite	2919	31.1	22.3	190
Dyke	3001	46.3	29.1	224
Greenstone	2989	27.9	21.8	277
Ore	4531	125.6	18.5	91
Metasediments	2768	11.0	7.9	146
Backfill	2000	0.2	0.1	2

Pre-mining stresses in the model are generated using boundary tractions, a method first developed by

McKinnon (2001) for a homogeneous rockmass, which was expanded subsequently for heterogeneous cases (Shnorhokian et al., 2014). Model calibration is conducted by comparing magnitudes of pre-mining stresses in the north dyke and norite formations with readings at comparable depth in the Canadian Shield.

3. STOPE SEQUENCE ALTERNATIVES

After pre-mining stress calibration is conducted, haulage drift-crosscut networks on all active levels are excavated simultaneously. Two stope sequences are then implemented between L 1550 and L 1430, comprising two simultaneous mining fronts. In the first one, operations commence from the eastern and western sides of the orebody and move towards the center and this is called the diminishing pillar option. In the second sequence, ore extraction starts from the middle and moves towards the sides and this is called the center-out approach. In both sequences, 6 stopes are extracted and backfilled per stage for a total of 24 stages to mine the orebody on all the active levels.

4. INSTABILITY CRITERIA

In order to examine potential instability around the drifts and crosscuts, two criteria are used from the literature related to failure mechanisms and mining-induced seismicity generation (McCreary et al., 1993; Trifu and Shumila, 2002). The brittle shear ratio (BSR) was developed by several authors (Castro et al., 1997; Martin et al., 1999) as an indicator for potential strainbursts. It compares the differential stress (σ_1 - σ_3) around an opening to the unconfined compressive strength (UCS) of intact rock. A ratio above 0.7 is indicative of major strainburst and damage potential (Castro et al., 2012). A second criterion used is the low compressive-tensile stress state (Diederichs and Kaiser, 1999; Diederichs, 2003), and values below 0.5 MPa are considered to represent rockmass failure for this study. The analysis focuses on a single active level – from L 1490 to L 1460 – for a quantitative comparison of the instability criteria for all 24 stages.

5. RESULTS AND DISCUSSIONS

5.1 Brittle shear ratio (BSR)

Table 2 presents the volume of rockmass above BSR 0.7 for the central formations between L 1490 and L 1460 in the diminishing pillar and center-out sequences. It also provides the volume of mined-and-backfilled stopes between these levels at Stages 4, 8, 12, 16, and 20, with all the ore having been extracted at Stage 24.

From the results, it can be observed that only the orebody exhibits BSR values above the 0.7 threshold. Figure 3 presents the locations of potentially unstable rockmass at Stage 8 in the diminishing pillar option, and they are seen to coincide with the two advancing mining fronts. While its rockmass properties indicate that the orebody is stiff, its relatively low UCS value also contributes to elevated BSR readings. Similarly, regions of unstable rockmass are confined to mining fronts in the center-out sequence, advancing from the center to the sides.

Table 2a: Diminishing pillar: volume (m^3) > BSR 0.7.

Geology	Drift	Stage 4	Stage 8	Stage 12	Stage 16	Stage 20
GS	0	0	0	0	0	0
Dyke	0	0	0	0	0	0
Ore	0	1875	11305	10397	18206	20323

Table 2b: Center-out: volume (m^3) > BSR 0.7.

Geology	Drift	Stage 4	Stage 8	Stage 12	Stage 16	Stage 20
GS	0	0	0	0	0	0
Dyke	0	0	0	0	0	0
Ore	0	2268	13988	15634	21608	15259

Table 2c: Volume of total ore mined at each stage ('000 m^3).

Geology	Stage 4	Stage 8	Stage 12	Stage 16	Stage 20	Stage 24
Ore	324	270	216	162	54	0
Backfill	0	54	108	162	270	324
Total	324	324	324	324	324	324

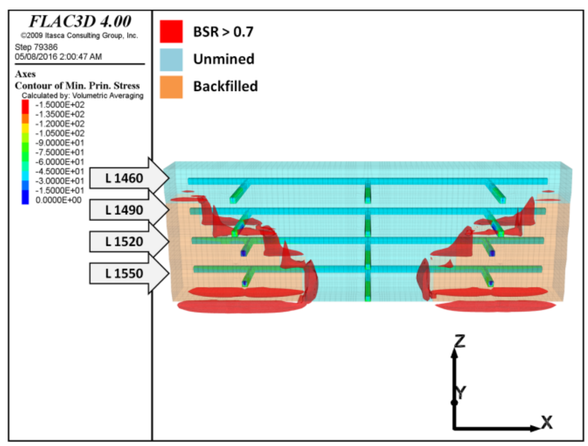

Figure 3: Stage 8 – diminishing pillar: BSR > 0.7.

While volumes of rockmass above a BSR of 0.7 indicate zones of potential mining-induced seismicity for the mining operation, the only development segments adjacent to them are those crosscuts that extend into the stopes. As the mining fronts advance, the eastern and western crosscuts on L 1490 are engulfed with potentially unstable rockmass at Stage 8 in the diminishing pillar sequence and at Stage 12 in the center-out one as shown in Figure 4.

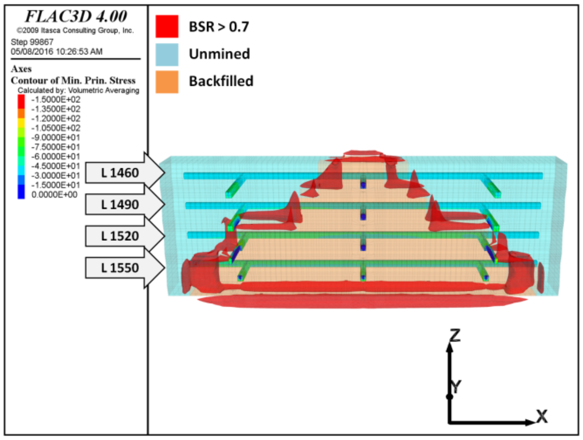

Figure 4: Stage 12 – center-out: BSR > 0.7.

When mining is confined to L 1550 and L 1520 in the initial stages, a relatively small volume of BSR instability (~ 1875 m^3) is detected on the study level between L 1490 and L 1460 in the diminishing pillar sequence. This value increases to almost 11300 m^3 at Stage 8 as the mining front reaches L 1490 and remains within the same range at Stage 12 (~ 10400 m^3). In the center-out option, larger volumes of unstable rockmass with elevated BSR conditions persist at all times except towards the end at Stage 20. In both mining sequences, regions of instability always coincide with the locations of the mining fronts. Hence, the center-out option exhibits more unstable rockmass at the onset of mining when the fronts are close to each other in the middle of the orebody, and registers a significant drop at Stage 20 when they have moved to its sides. In a reverse trend, the diminishing pillar sequence shows a slightly lower volume of unstable rockmass at the onset when the mining fronts are at the sides, and the volume of instability increases to a maximum at Stage 20 when the mining fronts form a pillar of minimum width in the center.

The expected effect of unstable rockmass with elevated BSR values is an increase in mining-induced seismicity. There is a general potential for rockbursts in the crosscuts at all times but a more specific risk of potential failure appears once the zone of influence of unstable rockmass reaches the excavation (Figures 3 and 4).

5.2 Low compressive and tensile stress

Table 3 presents the volumes of potentially unstable rockmass under low compressive and tensile stress conditions. When compared to the previous one, the extent is observed to be more widespread. The volumes of unstable rockmass in the orebody are comparable to the ones with the BSR criterion, and fluctuate with mining operations until Stage 24. The difference is that the volumes with a potential low compression or tensile stress instability mechanism extend to the greenstone unit that forms the footwall and immediate hanging wall on either side of the orebody. Hence, they are no longer restricted to the mining fronts only as can be observed in Figure 5. In addition, the unstable rockmass volumes within the greenstone formation continuously rise with each mining stage until the end.

Table 3a: Diminishing pillar: volume (m^3) of σ_3 < 0.5 MPa.

Geology	Stage 4	Stage 8	Stage 12	Stage 16	Stage 20	Stage 24
GS	0	3987	13614	19493	32484	16629
Dyke	0	0	0	0	0	0
Ore	1369	13127	6299	11055	11020	0

Table 3b: Center-out: volume (m^3) of σ_3 < 0.5 MPa.

Geology	Stage 4	Stage 8	Stage 12	Stage 16	Stage 20	Stage 24
GS	0	5349	14738	17289	23099	16551
Dyke	0	0	0	0	0	0
Ore	2392	11254	5716	12262	9919	0

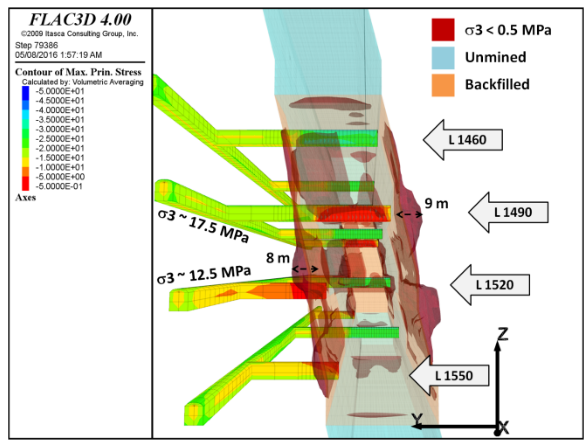

Figure 5: Stage 8 – diminishing pillar: σ_3 < 0.5 MPa.

In the hanging wall, these regions constitute potential volumes of unplanned dilution that could move into the stope once it is mined out. In the footwall, unplanned dilution is still a possibility at the top of the study level near L 1460. However, sections near the bottom that are close to crosscuts represent potential instability and fall-of-ground, especially in the roofs. It is not only the temporary section of a crosscut within a given stope that is at potential risk, as was the case with the BSR criterion. Rather, the remaining section within the greenstone footwall is also affected by the volume of unstable rockmass. The western crosscut on L 1490 is shown in Figure 6 with an outline of rockmass under low compressive and tensile stress above it. Important quantitative parameters such as the volume of potential failure, its location in the roof of the crosscut, and distance from the orebody can be calculated easily based on this analysis, as shown in Figure 5 and 6. Similarly, the extent of potential unplanned dilution that may affect the hanging wall on the level below is seen in the same figures.

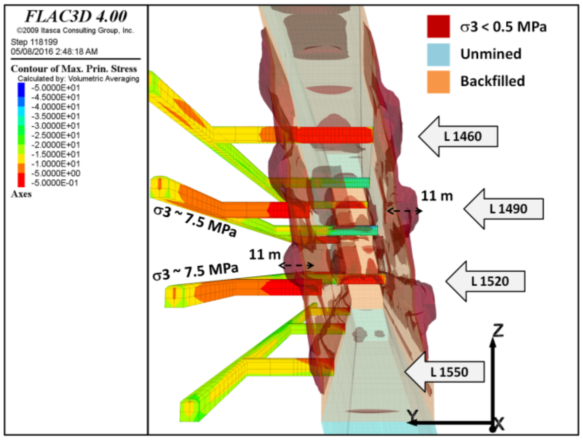

Figure 6: Stage 16 – diminishing pillar: $\sigma_3 < 0.5$ MPa.

One of the advantages of a quantitative analysis is that volumes of unstable rockmass in different locations can be assessed regarding their impact on mining operations. The volume in the greenstone unit can be subdivided into its footwall and hanging wall components with the latter representing between 43 and 48% of the total unstable rockmass during all mining stages in the diminishing pillar sequence (Table 4a). Thus, it quantifies the unplanned ore dilution that can potentially be expected from the hanging wall. It follows that between 52 and 57% of the unstable rockmass is located in the footwall, and these volumes can act as sources of potential dilution and crosscut instability.

Table 4a: Diminishing pillar: volume (m^3) of $\sigma_3 < 0.5$ MPa.

Geology	Stage 4	Stage 8	Stage 12	Stage 16	Stage 20	Stage 24
GS	0	3987	13614	19493	32484	16629
HW	0	1906	5908	8797	14092	5514
FW	0	2081	7706	10696	18392	11114

Table 4b: Center-out: volume (m^3) of $\sigma_3 < 0.5$ MPa.

Geology	Stage 4	Stage 8	Stage 12	Stage 16	Stage 20	Stage 24
GS	0	5349	14738	17289	23099	16551
HW	0	2393	5625	7323	7921	6864
FW	0	2957	9114	9965	15178	9687

Table 4b presents the same data for the center-out sequence and a simple comparison between the two indicates important trends. In terms of hanging wall instability, the volumes are consistently smaller in the center-out option from Stage 12 onward but higher at Stage 8. The footwall side shows smaller volumes for this sequence from Stage 16 onward but higher numbers before. This phenomenon has a valid explanation related to the location of mining fronts. In the diminishing pillar approach, mining proceeds from the sides to the center and instability increases in volume as the pillar develops there. In the center-out option, operations commence from the center and the largest volumes of instability can be observed at the beginning (Stages 8 and 12) when both mining fronts are in close proximity in the center.

Another trend observed is the relative volumes of unstable rockmass in the greenstone formation once mining operations end. While the total numbers are comparable, the diminishing pillar option ends with a much more voluminous instability in the footwall (67%) than in the hanging wall (33%). Although the footwall has a higher volume of unstable rockmass in the center-out option as well at 59%, compared to the 41% in the hanging wall, the distribution is a more balanced one.

6. CONCLUSIONS

A conceptual model is constructed in FLAC^{3D} for a typical tabular, steeply dipping orebody in the Canadian Shield that uses the sublevel open stoping method. A series of drifts and crosscuts are replicated on four active levels and two stope sequences with two simultaneous mining fronts are implemented. In the first case, ore extraction moves from the sides to the center while the reverse takes place in the second one. The brittle shear ratio and low compressive-tensile stress state are used as instability criteria, and are coupled with volumetric analysis for quantitative comparisons. It is observed that in both sequences, the potential BSR instability zones are restricted to the orebody and mining fronts. However, zones under low compressive and tensile stress conditions can be found in the greenstone footwall and hanging wall, in addition to the stopes, and pose a risk to crosscuts. Their relative distribution between the footwall and hanging wall is observed to be a more balanced one in the center-out option than in the diminishing pillar sequence.

7. REFERENCES

Bieniawski, Z.T. (1989). Engineering rock mass classifications: a complete manual for engineers and geologists in mining, civil, and petroleum engineering. Wiley-Interscience, New York, 272 p.

Bullock, R.L. (2011). Comparison of underground mining methods. In: SME Mining Engineering Handbook, Darling P. (ed.), SME, pp. 385-403.

Cai, M. (2013). Principles of rock support in burst-prone ground. Tunnelling and Underground Space Technology, Volume 36, pp. 46-56.

Cai, M. and Kaiser, P.K. (2014). In-situ rock spalling strength near excavation boundaries. Rock Mechanics and Rock Engineering, Volume 47, pp. 659-675.

Castro, L.A.M., Grabinsky, M.W., McCreath, D.R. (1997). Damage initiation through extension fracturing in a moderately jointed brittle shear rock mass. International Journal of Rock Mechanics and Mining Sciences, Volume 34, No. 3-4, pp.110e.1-110.e13.

Castro L.A.M., Bewick R.P., and Carter T.G. (2012). An overview of numerical modelling applied to deep mining. In: Innovative numerical modelling in geomechanics, Azevedo R. (ed.), CRC Press – Taylor & Francis Group, pp. 393-414.

Diederichs, M.S. (2003). Rock fracture and collapse under low confinement conditions. Rock Mechanics and Rock Engineering, Volume 36, No. 5, pp. 339-381.

Diederichs, M.S. and Kaiser, P.K. (1999). Tensile strength and abutment relaxation as failure control mechanisms in underground excavations. International Journal of Rock Mechanics and Mining Sciences, Volume 36, pp. 69-96.

Diederichs, M.S., Kaiser, P.K., and Eberhardt, E. (2004). Damage initiation and propagation in hard rock during tunneling and the influence of near-face stress rotation. International Journal of Rock Mechanics and Mining Sciences, Volume 41, pp. 785-812.

Gay, N.C., Jager, A.J., Ryder, J.A., and Spottiswoode, S.M. (1995). Rock-engineering strategies to meet the safety and production needs of the South African mining industry in the 21st century. Journal of the South African Institute of Mining and Metallurgy, Volume 95, No. 3, pp. 115-136.

Grimstad, E. and Barton, N. (1993). Updating the Q-System for NMT. In: Proceedings of the International Symposium on Sprayed Concrete – Modern Use of Wet Mix Sprayed Concrete for Underground Support, Kompen, Opsahl, and Berg (eds.), Norwegian Concrete Association, pp. 46-66.

Hamrin, H. (1998). Choosing an underground mining method. In: Techniques in Underground Mining, Gertsch, R.E. and Bullock, R.I.(eds.), SME, pp. 45-85.

Hoek, E., Caranza-Torres, C.T., Corcum, B. (2002). Hoek-Brown failure criterion – 2002 edition. In: Proceedings of the North American Rock Mechanics Society (NARMS-TAC 2002), Bawden, H.R.W., Curran, J., and Telsenicki, M. (eds), pp. 267-273.

Itasca (2006). Itasca Software Products – FLAC^{3D}. Itasca Consulting Group Inc., Minneapolis.

Kaiser, P.K., Tannant, D.D., and McCreath, D.R. (1996). Drift support in burst-prone ground. CIM Bulletin, Voume 89, No. 998, pp. 131-138.

Kaiser, P.K., Diederichs, M.S., Martin, D., Sharpe, J. and Steiner, W. (2000). Underground works in hard rock tunnelling and mining. In: GeoEng2000, Technomic Publishing Company, pp. 841-926.

Kaiser, P.K., Yazici, S., and Maloney, S. (2001). Mining-induced stress change and consequences of stress path on excavation stability – a case study. International Journal of Rock Mechanics and Mining Sciences, Volume 38, No. 2, pp. 167-180.

Kendorski, F.S. (1993). Some modes of deformation and failure of lined tunnels. International Journal of Rock Mechanics and Mining Sciences Abstracts, Volume 30, No. 7, pp.1497-1501.

Martin, C.D., Kaiser, P.K., and McCreath, D.R. (1999). Hoek-Brown parameters for predicting the depth of brittle failure around tunnels. Canadian Geotechnical Journal, Volume 36, No. 1, pp. 136-151.

McCreary, R.G., Grant, D., and Falamagne, V. (1993). Source mechanisms, three-dimensional boundary-element modelling, and underground observations at Ansil Mine. In: Proceedings of the 3rd International Symposium on Rockburst and Seismicity in Mines, Young, R.P. (ed.), pp. 227-232.

McKinnon, S.D. (2001). Analysis of stress measurements using a numerical model methodology. International Journal of Rock Mechanics and Mining Sciences, Volume 38, pp. 699-709.

Shnorhokian, S., Mitri, H.S., and Thibodeau, D. (2014). A methodology for calibrating numerical models with a heterogeneous rockmass. International Journal of Rock Mechanics and Mining Sciences, Volume 70, pp. 353-367.

Shnorhokian, S., Mitri, H.S., and Moreau-Verlaan, L. (2015). Stability assessment of stope sequence scenarios in a diminishing ore pillar. International Journal of Rock Mechanics and Mining Science, Volume 74, pp. 103-118.

Trifu, C.I. and Shumila, V. (2002). Reliability of seismic moment tensor inversions for induced microseismicity at Kidd Mine, Ontario. Pure and Applied Geophysics, Vol. 159, pp. 145-164.

Zhang, Y. and Mitri, H.S. (2008). Elastoplastic stability analysis of mine haulage drift in the vicinity of mined stopes. International Journal of Rock Mechanics and Mining Science, Volume 45, pp. 574-593.